行政院國家科學委員會專題研究計畫　成果報告

瞬間正則模分析液体水內分子動力學之研究(2/2)

計畫類別：個別型計畫
計畫編號：NSC91-2112-M-009-035-
執行期間：91 年 08 月 01 日至 92 年 07 月 31 日
執行單位：國立交通大學物理研究所

計畫主持人：吳天鳴

計畫參與人員：張士良(博士研究生)

報告類型：完整報告

處理方式：本計畫涉及專利或其他智慧財產權，1 年後可公開查詢

中　華　民　國 92 年 10 月 27 日

I Introduction

Although water has been studied for a long time, the microscopic dynamics is still little known for its complexity in hydrogen-bond network. In experiments, infrared and Raman spectroscopy give little information because the corresponding line shapes of water are strongly inhomogeneously broadened by the strong variation in hydrogen-bond interactions, including hydrogen-bond bend and streth vibrations, and librational motion. Recently, in terms of the pump-probe technique of ultrafast spectroscopy, it is possible to resolve the inhomogeneous absorption band of water [1]. In a femtosecond mid-infrared experiment with such technique for HDO molecules dissolved in liquid D_2O [2, 3], the HDO molecules are selected by the pump frequency, within the absorption band of the OH stretch vibration, and, then, the orientational motion of the selected HDO molecules, which form a subensemble in liquid water, is probed with the measurement of the anisotropy parameter as a function of the delay time between the pump and the probe pulses. The experimental results show that the orientational relaxation of water molecules depends on the pump frequency, with faster relaxation dacay for higher pump frequency. It is generally believed that the OH stretch vibrational frequency is strongly influenced by the length of the O-H...O hydrogen bond between the OH group and the O atom of a neighboring D2O molecule, with a tendency that the shorter the length, the

lower the frequency [4]. Thus, this experiment indicates that the orientational motion of a molecule in liquid water is determined by the strengths of the hydrogen bonds connected to the molecule, and the the effective orientation rate in liquid water is governed by the fraction of the water molecules for which orientation is not hindered by the O-H...O hydrogen bond. .

Though the experiment is greatly successful, the study at molecular level of how the orientational motions in liquid water are related to the network of the hydrogen bonds is still in the infant stage. To understand the orientational dynamics of liquid water is essentially important for realizing the physical and chemical processes that happen in this liquid. Computer simulation is one of the powerful method to do this study. In this project, in terms of molecular dynamics (MD) simulations, we have done the instantaneous-normal-mode (INM) analysis for the orientational motions of subensemble molecules in liquid water, which are classified according to the hydrogen bonds connected to a molecule and the geometry around a molecule.

In a previous report, we have presented the INM analysis for the orientational motions of the SPC/E model with rigid water molecule, classified into subensembles by the Voronoi polyhedra analysis and the hydrogen-bond configurations. In this report, based on the SPC/E model, we extend to a flexible model [13], in which anharmonic potential is used for the OH bond in a molecule. The Voronoi polyhedra analysis is applied in the study

of the INM density of states (DOSs). The organization of this report is as following. In section II, we describe the INM method on the flexible model and combine them with the Voronoi polyhedra analysis as what we did in the previous report. Also, the velocity autocorrelation functions of the hydrogen and oxygen and their fittings with the INM method are discussed. In section III, we describe our MD simulations first. After that, the results of the INM DOSs and velocity autocorrelation functions are presented. Finally, our conclusions are given in section IV.

II The instantaneous normal mode analysis

Consider N water molecules in a cubic box with length L. The total Hamiltonian of this system can be written as

$$H = \sum_{j,\alpha} \frac{1}{2} m_{j,\alpha} \dot{r}_{j,\alpha}^2 + V, \tag{1}$$

where $\mathbf{r}_{j,\alpha}$ and $m_{j,\alpha}$ denote the position and mass of α^{th} atom of molecule j, respectively. V is the interactions, which include the Coulomb and Lennard-Jones interactions, V_C and V_{LJ}, between two water molecules, respectively, and the intramolecular interactions V_{Intra}.

Let $\dot{\mathbf{z}}_{j,\alpha} \equiv m_{j,\alpha}^{1/2}\dot{\mathbf{r}}_{j,\alpha}$ and expand V up to the second order of displacements, the total Hamiltonian can be approximated to be

$$H = \sum_{j,\alpha} \frac{1}{2}\dot{z}_{j,\alpha}^2 + V_0 - \mathbf{F}(\mathbf{Z}_0)\cdot(\mathbf{Z}_t - \mathbf{Z}_0) + \frac{1}{2}(\mathbf{Z}_t - \mathbf{Z}_0)\cdot\mathbf{D}(\mathbf{Z}_0)\cdot(\mathbf{Z}_t - \mathbf{Z}_0). \tag{2}$$

Here,

$$\mathbf{Z} \equiv \{\mathbf{z}_{1,H_1}, \mathbf{z}_{1,H_2}, \mathbf{z}_{1,O}, \ldots, \mathbf{z}_{N,H_1}, \mathbf{z}_{N,H_2}, \mathbf{z}_{N,O}\} \tag{3}$$

and the subscript t and 0 of $\mathbf{Z}$ denote that $\mathbf{Z}$ is evaluted at time t and 0, respectively. $\mathbf{F}$ and $\mathbf{D}$ are the $9N$-dimensional force vector and the $9N \times 9N$ Hessian matrix, which are defined as

$$F_{j,\alpha,\mu} = -\frac{\partial V}{\partial z_{j,\alpha,\mu}}, \tag{4}$$

$$D_{j,\alpha,\mu,k,\beta,\nu} = \frac{\partial^2 V}{\partial z_{j,\alpha,\mu}\partial z_{j,\beta,\nu}}, \tag{5}$$

where μ and ν denote x, y, or z.

If $\mathbf{D}$ is diagonalized through an orthogonal transformation of $\mathbf{U}$, the density of state

(DOS) and the projector P_β^α are defined as

$$D(\omega) = \left\langle \frac{1}{9N} \sum_{\beta=1}^{9N} \delta(\omega - \omega_\beta) \right\rangle, \tag{6}$$

$$P_\beta^\alpha = \sum_{j=1\ldots N, \mu=x,y,z} U_{\beta,j\alpha\mu}^2. \tag{7}$$

With P_β^α, where α can be H for hydrogen atom and o for the oxygen atom, the DOS can be separated into two parts: one contributed from the oxygen atoms, the other from the hydrogen atoms. Therefore, we have $D(\omega) = 2D_H(\omega) + D_O(\omega)$, where

$$D_\alpha(\omega) = \left\langle \frac{1}{9N} \sum_{\beta=1}^{9N} \delta(\omega - \omega_\beta) P_\beta^\alpha \right\rangle. \tag{8}$$

In the previous chapter, water molecules are classified into different Voronoi groups (VGs) according to their asppericity η, which is defined as $\eta = A^3/36\pi V^2$. Here, A and V are the volume and total surface of the Voronoi unit cell, respectively. By the similar way in the previous chapter, Voronoi unit cells are constructed by the oxygen atoms of the water molecules. Each water molecule is classified into one of the four groups according to its Voronoi asphericity. For different VGs, the corresponding projector and DOS can

be written as

$$P_{\beta}^{\alpha\eta} = \sum_{j=1...N,\mu=x,y,z} \Theta_{\eta}(j) U_{\beta,j\alpha\mu}^{2}, \tag{9}$$

$$D_{\alpha\eta}(\omega) = \left\langle \frac{1}{9N} \sum_{\beta=1}^{9N} P_{\beta}^{\alpha\eta} \delta(\omega - \omega_{\beta}) \right\rangle. \tag{10}$$

Here, $\Theta_{\eta}(j) = 1$ if molecule j is in the VG η and zero otherwise.

Usually, the velocity autocorrelation functions can be calculated by the DOS. Here, we define the velocity autocorrelation functions of the oxygen and hydrogen atoms (VAFO and VAFH), respectively, as

$$C_{v\alpha}(t) = \frac{< \mathbf{v}_{\alpha}(t) \cdot \mathbf{v}_{\alpha}(t) >}{< \mathbf{v}_{\alpha}(0) \cdot \mathbf{v}_{\alpha}(0) >}. \tag{11}$$

As usual, the VAFO and VAFH can be fitted by the INM DOS with the following formula

$$C_{v\alpha}(t) = \int_{-\infty}^{\infty} D_{\alpha}(\omega) \cos(\omega t) d\omega. \tag{12}$$

Similar formula are also applied for the VAF of different VGs, with the DOS replaced by the corresponding one.

III Results and discussions

III.1 The molecular dynamics simulation

Properties of liquid water have been widely studied through molecular dynamics simulations[5][6]. At first, simplified models with rigid molecules are used. Based on these rigid models, many intermolecular potentials and extensions have been proposed[7][8]. Many properties, both in structures and dynamics, calculated from these rigid models agree well with experimental data. However, it is still an open question whether the rigid models can stand for a real water system [9][10]. Further, some properties, intramolecular vibrations for example, can not be examined with the rigid models.

Recently, to include the intramolecular vibrational motions[11], the intramolecular potential in a Morse form has been used for extending the rigid model based on the SPC model[7]. New properties, including the O-H bond distance, vibration spectra, and etc, have been studied. In addition to the flexible model in Ref. [11], many different flexible models have also been proposed. These models are based on the SPC/E model, by adding the harmonic HOH bending and the anharmonic OH stretching potentials [12][13]. The PJT2 model developed by Polyansky et al.[14] is one of the models. In the PJT2 model, the energies of 3200 experimentally observed rotation-vibrartion levels are used for fitting the parameters of the model and it is highly accurate in describing the intramolecular

vibrations of water molecules.

Through the spectroscopy studies [16] with the flexible models, the interactions between the vibrational and the rotational motions can be neglected [15]. The flexible SPC model[17] in Ref. [16], which is modified from the model in Ref. [11], has produced better agreements in the IR (infrared) spectra. These studies suggest a clearly separtion in time scales between the correlation of the dipole moment due to rotational motions and the vibrational motions.

The flexible model has been studied by the instantaneous-normal-mode (INM) method[18][19]. Also, the INM spectra and the spectra of the time correlation functions are compared. Besides the purely classical mechanical model, a quantum mechanical path integral calculation is used in the INM analysis and is termed as QINM. However, the results from the QINM method is worse than those from the INM in purely classical mechanical model. This suggests that purely classical mechanical models can be superior to mixing classical and quantum treatments. This is also suggested by Bader and Berne[20].

In our simulations, we consider a system of 256 water molecules in a cubic box with box length L and the periodic boundary conditions. The flexible water model in Ref.[13], based on the SPC/E model, is used and the Ewald sum rule is also applied. In our flexible SPC/E model, the Lennard-Jones part for the oxygen-oxygen interaction is truncated at

$L/2$ and the potential is shifted upward such that it is continuous at the truncated point. The leap-frog algorithm is used for integrating the equations of motion with time step equal to 0.2 fs.

Before simulations, the molecules in the initial states form a fcc lattice structure and have randomly distributed velocities, which are satisfied with the Maxwell-Boltzmann distribution. We discarded the first 300,000 time steps to make sure that the equilibrium state is reached, and then started to take data. The thermodynamic state in our simulations here is at density $\rho = 1.0\ g/cm^3$ and temperature $T = 300\ K$.

III.2 Structures

In Fig. 1, the oxygen-oxygen, oxygen-hydrogen, and hydrogen-hydrogen radial distribution functions, which are denoted as $g_{OO}(r)$, $g_{OH}(r)$, and $g_{HH}(r)$, respectively, are shown. Our MD results have been carefully compared with the corresponding pair distribution functions in Ref. [13] to make sure the correctness of our MD simulation. For the flexible SPC/E model, the first maxima the $g_{OO}(r)$, $g_{OH}(r)$, and $g_{HH}(r)$ are all found to be a little higher and the first-shell widths to be a little narrower than those of the rigid SPC/E model. This suggests that in the flexible SPC/E model the extra vibrational degrees of freedom, which allow the deformation of each molecule, make the liquid a little

more compact in structure; however, the difference is not much.

In Fig. 2, $g^{\eta}_{OO}(r)$, $g^{\eta}_{OH}(r)$, and $g^{\eta}_{HH}(r)$ of different VGs are shown. From these pair distribution functions, similar results occurring in the rigid model, including the more random structure in VG I, the highly ordered structure in VG IV, more broken HBs in VG I, isosbestic points which suggest the mixutre of two-state local structures in liquid water, are also found in the flexible SPC/E model. In general, there are little differences in strucutre between the rigid and flexible SPC/E models. Therefore, the general conclusions we gave in the previous report about the structures of liquid water are still available for the flexible SPC/E model.

III.3 The instantaneous normal modes

The INM DOS of the flexible SPC/E model is shown in Fig. 3. A distinct difference between the DOSs of the flexible SPC/E model and that of the rigid model is the high-frequency modes due to the intramolecular potential. For the flexible model, two high-frequency regions, with their mean frequencies at 1660 and 3480 cm^{-1}, are found. These two spectra are associated with the bending (1660 cm^{-1}) and stretching (3480 cm^{-1}) intramolecular motions of liquid water [18]. These are consistent with the experimental bending (1670 cm^{-1}) and stretching (3557 cm^{-1}) frequencies[12]. In the meanwhile, the

mean frequency of the rotational DOS of the flexible model is a little higher than that of the rigid model in both the real and the imaginary lobes, while the translational DOSs are almost the same for both models. In terms of the projector P_β^α, the DOS can be separated into $D_H(\omega)$ and $D_O(\omega)$. Not surprising, $D_O(\omega)$ is dominated at the low-frequency region, while $D_H(\omega)$ contributes at the high-frequency region. This is consistent with the interpretation for the translational DOS, which is partly due to the O-O-O bending motions[21][22].

For different VGs, their corresponding DOSs are shown in Fig. 4. For the imaginary spectra of $D_H(\omega)$, the decreasing in the fraction and the blue shift (to higher frequencies) with the increasing in the asphericity of a VG are found. The blue shift can be understood to be due to the difference in the strengeh of the hydrogen bonding. On the real-frequency side, the translational and the bending spectra are found to be blue-shift with the increasing in asphericity; however, the stretching spectrum to be red-shift. These are consistent with the frequency shifts between the water monomer and liquid water. For $D_O(\omega)$, not only the decreasing in the fraction of the imaginary INMs is found, but also a bump at about $300cm^{-1}$ in the real-frequency lobe is shown.

With $D_O(\omega)$ and $D_H(\omega)$, the oxygen and the hydrogen velocity autocorrelation functions, $C_{vO}(t)$ and $C_{vH}(t)$, can be predicted by the INM approach. Since $D_H(\omega)$ has a significant contribution to both the bending and the stretching branches, there should

be many high-frequency oscillations in $C_{vH}(t)$. On the other hand, $D_O(\omega)$ in the high-frequency region is relatively small. This suggests that the high-frequency oscillations in $C_{vO}(t)$ are small in amplitude. In Fig. 5, we show the INM approximations of $C_{vH}(t)$ and $C_{vO}(t)$. Clearly, high-frequency oscillations are observed in $C_{vH}(t)$, while the corresponding oscillations are insignificant in $C_{vO}(t)$.

III.4 Rotational Dynamics

The rotational dynamics can be studied via the rotational autocorrelation function which is defined as

$$C_2(t) =< P_2(\mathbf{e}(t) \cdot \mathbf{e}(0)) >, \tag{13}$$

where $\mathbf{e}$ is the unit vector of certain molecular direction and $P_2(x)$ is the second-order Legendre polynomial. For the unit vector along the dipole moment of a water molecule, we present the comparison between the $C_2(t)$ autocorrelation functions of the rigid and the flexible models in Fig. 6, in which curves are averaged for all molecules, and in Fig. 7, in which curves are averaged for molecules in different Voronoi groups.

IV Conclusion

Both MD simulations and the INM method have been used to investigate the differences in structures and dynamics between the flexible and the rigid SPC/E models. Most conclusions in structures we got in the rigid model are also available in the flexible SPC/E model, except that the structures in the structures in the flexible SPC/E model become more ordered. However, in dynamics, the flexible SPC/E model provides the informations about the bending and stretching motions in liquid water, which are missing in the rigid SPC/E model.

For different VGs, features found in the rigid model, including the isobestic points in pair distribution functions, the blue shift in the rotational spectra with the increasing of asphericity, and etc, are also found in the flexible SPC/E model. For the flexible SPC/E model, we also found a blue and a red shift in the bending and the stretching spectra with the increasing of asphericity, respectively.

References

[1] S. Woutersen, U. Emmerichs, and H. J. Bakker, Science **278**, 658 (1997).

[2] H. J. Bakker, S. Woutersen, and U. Emmerichs, Chem. Phys. **258**, 233 (2000).

[3] H. K. Nienhuys, R. A. van Santen, and H. J. Bakker, J. Chem. Phys. **112**, 8487 (2000).

[4] C. P. Lawrence and J. L. Skinner, J. Chem. Phys. **118**, 264 (2003).

[5] A. Rahman and F. H. Stillinger, J. Chem. Phys. **55**, 3336 (1971).

[6] D. M. Heyes, J. Chem. Soc. Faraday Trans. **90**, 3039 (1994).

[7] W. L. Jorgensen, J. Chandrasekhar, J. D. Madura, R. W. Impey, and M. L. Klein, J. Chem. Phys **79**, 926 (1983).

[8] H. J. C. Berendsen, J. R. Grigera, and T. P. Straatsma, J. Phys. Chem. **91**, 6269 (1987).

[9] J. L. Barrat and I. R. McDonald, Molecular Physics **70**, 535 (1990).

[10] O. Teleman, B. Jönsson, and S. Engström, Molecular Physics **60**, 193 (1987).

[11] K. Toukan and A. Rahman, Phys. Rev. B **31**, 2643 (1985).

[12] D. M. Ferguson, J. of Comp. Chem. **16**, 501 (1995).

[13] M. E. Parker and D. M. Heyes, J. Chem. Phys. **108**, 9039 (1998).

[14] O. L. Polyansky, P. Jensen, and J. Tennyson, J. Chem. Phys. **105**, 6490 (1996).

[15] E. B. Wilson, J. C. Decius, and P. C. Cross, Molecular Vibrations, Dover Publications Inc., New York (1955).

[16] J. Martí and J. A. Padrò, Molecular Simulation **23**, 55 (1999).

[17] J. Martì, J. A. Padrò, and E. Guàrdia, J. of Mol. Liq. **62**, 17 (1994).

[18] H. Ahlborm, X. D. Ji, B. Space, and P. B. Moore, J. Chem. Phys. **111**, 10622 (1999).

[19] H. Ahlborn, B. Space, and P. B. Moore, J. Chem. Phys. **112**, 8083 (2000).

[20] J. S. Bader and B. J. Berne, J. Chem. Phys. **100**, 8359 (1994).

[21] F. Sciortino and S. Sastry, J. Chem. Phys. **100**, 3881 (1994).

[22] M. G. Sceats, M. Stavola, and S. A. Rice, J. Chem. Phys. **70**, 3927 (1979).

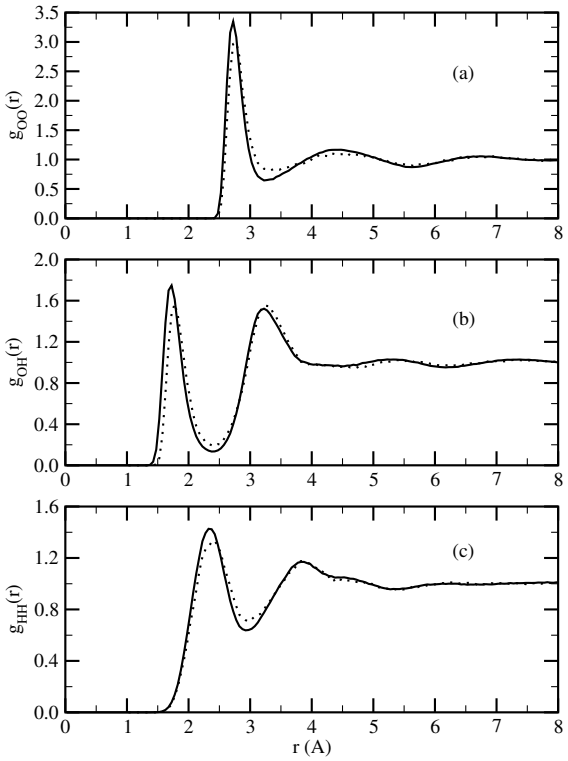

Figure 1: The oxygen-oxygen (a), oxygen-hydrogen (b), and hydrogen-hydrogen (c) raidal distribution functions at density $\rho = 1g/cm^3$ and temperature $T = 300K$. The solid and dot lines are for the pair distribution functions of the flexible and rigid models, respectively.

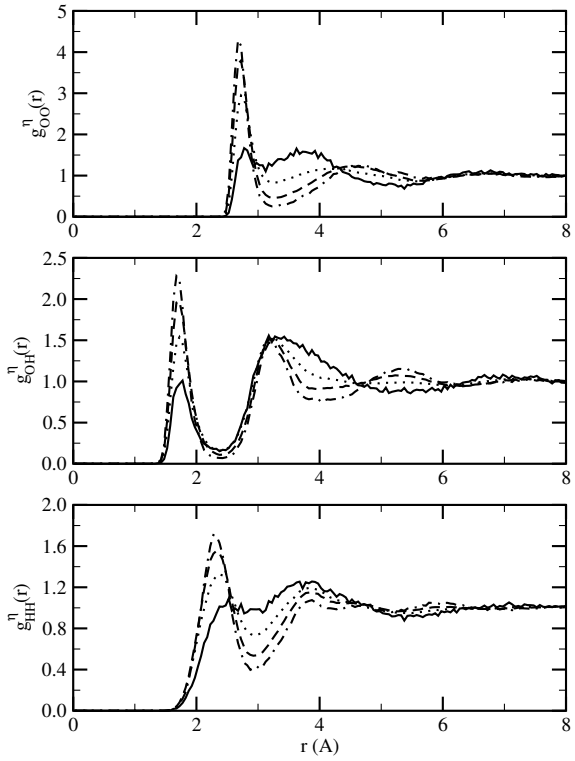

Figure 2: $g_{OO}(r)$, $g_{OH}(r)$, and $g_{HH}(r)$ of different VGs. The VG I, II, III, IV are represented by the solid, dot, dash, and dot-dash lines, respectively.

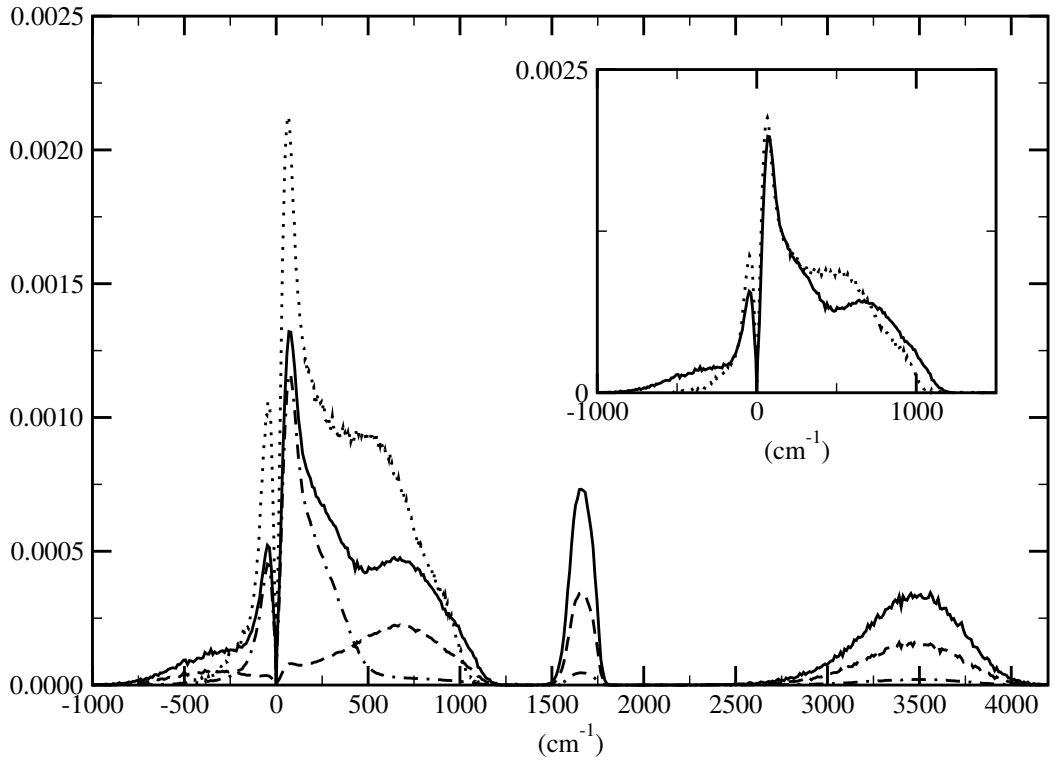

Figure 3: The INM DOS for the flexible (solid line) and the rigid (dot line) models. The DOS projected on the hydrogen and oxygen atoms are denoted by the dash and dot-dash lines, respectively. In the inset, The contribution from the intermolecular interactions in the DOS of the flexible model (solid line) is compared with the DOS of the rigid model (dot line), with both being normalized to unity.

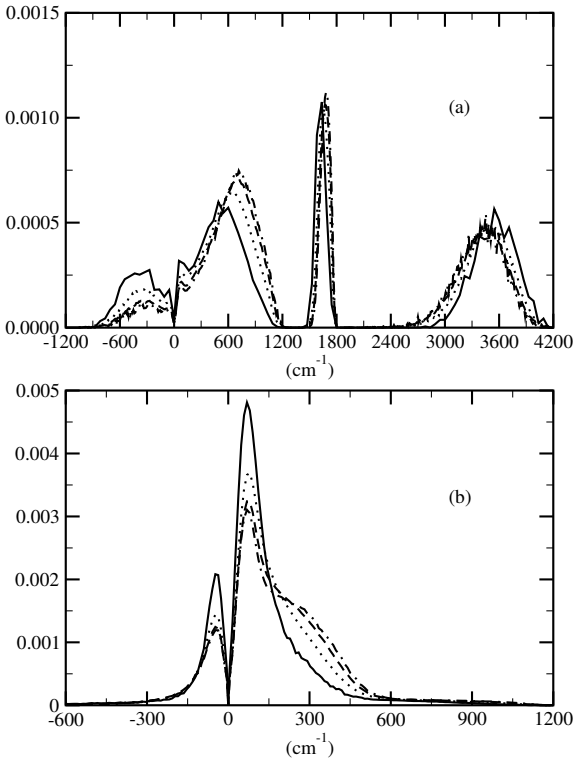

Figure 4: $D_H(\omega)$ (a) and $D_O(\omega)$ (b) for different VGs. The corresponding DOS of VG I, II, III, and IV are represented by the solid, dot, dash, and dot-dash lines, respectively.

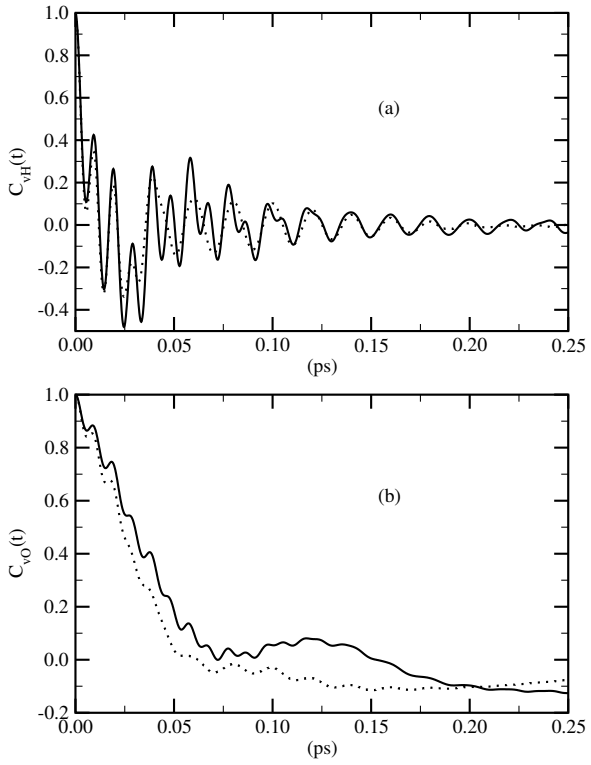

Figure 5: The hydrogen and oxygen velocity autocorrelation functions. The solid and the dot lines are the simulation results and the INM calculations, respectively.

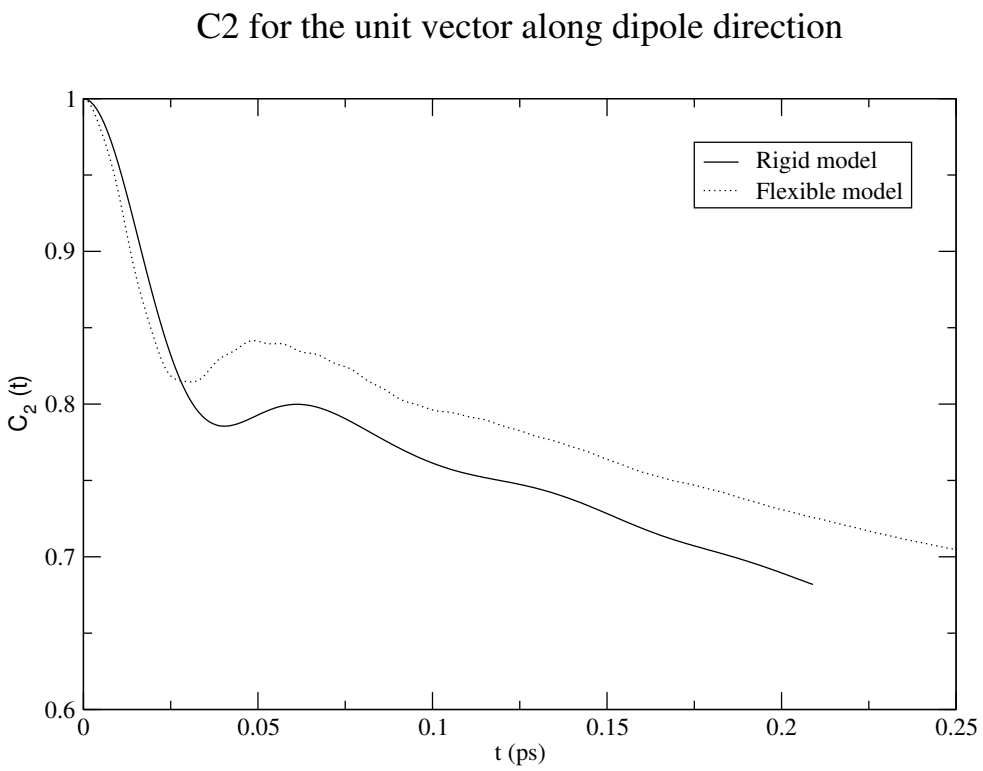

Figure 6: The autocorrelation function of $C_2(t)$ for unit vector along the dipole moment direction. The solid and the dot lines are for the rigid and the flexible models, respectively.

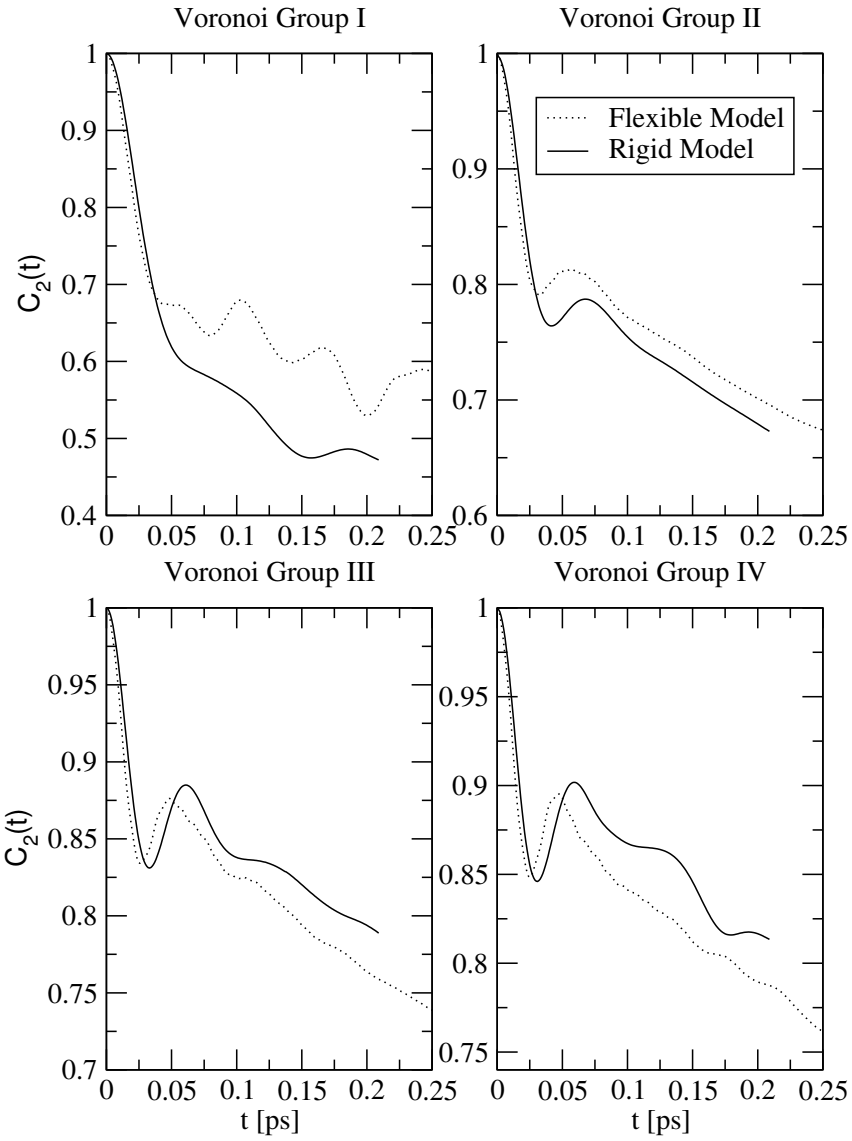

Figure 7: The autocorrelation functions similar in Fig. 6 but for water molecules in different Voronoi groups.